Communication: Nonadiabatic ring-polymer molecular dynamics

Jeremy O. Richardson, and Michael Thoss

Citation: The Journal of Chemical Physics **139**, 031102 (2013); doi: 10.1063/1.4816124
View online: https://doi.org/10.1063/1.4816124
View Table of Contents: http://aip.scitation.org/toc/jcp/139/3
Published by the American Institute of Physics

THE JOURNAL OF CHEMICAL PHYSICS **139**, 031102 (2013)

Communication: Nonadiabatic ring-polymer molecular dynamics

Jeremy O. Richardson and Michael Thoss
Institut für Theoretische Physik und Interdiziplinäres Zentrum für Molekulare Materialien, Friedrich-Alexander-Universität Erlangen-Nürnberg, Staudtstr. 7, 91058 Erlangen, Germany

(Received 4 June 2013; accepted 5 July 2013; published online 19 July 2013)

A new method based on an extension of ring-polymer molecular dynamics is proposed for the calculation of thermal correlation functions in electronically nonadiabatic systems. The ring-polymer dynamics are performed using a continuous-variable representation of the electronic states within the mapping approach, such that the electronic and nuclear degrees of freedom are treated on an equal footing. Illustrative applications of the method show good agreement with exact quantum results for the dynamics over short to moderate times and reveal a systematic improvement over the classical implementation of the mapping approach (single-bead limit). Being based on trajectories, the method scales well with the number of degrees of freedom and will be applicable to simulate certain nonadiabatic processes in complex molecular systems. © *2013 AIP Publishing LLC*. [http://dx.doi.org/10.1063/1.4816124]

INTRODUCTION

A long-standing goal in theoretical chemistry is the accurate simulation of electronically nonadiabatic processes in complex molecular systems.[1–5] While fully quantum-mechanical methods can provide numerically exact descriptions of such processes, approximate trajectory-based methods are typically computationally less demanding and can be combined with an on-the-fly calculation of the potential energy, thus avoiding the precalculation of multidimensional potential energy surfaces. A variety of trajectory-based methods for nonadiabatic dynamics have been developed in the last decades including (quasi)classical, mixed quantum-classical, and semiclassical approaches.[6] In this paper, we propose a novel approach to electronically nonadiabatic dynamics, which is based on an extension of the ring-polymer molecular dynamics (RPMD) method.

The RPMD method is an approximate quantum-dynamical approach based on the imaginary-time path-integral formulation of the Boltzmann operator[7] in statistical mechanics. The method was originally developed for the simulation of dynamical processes which can be described by a single potential energy surface, i.e., where the Born-Oppenheimer approximation is valid.[8] For such systems, RPMD provides directly an approximation to Kubo-transformed thermal correlation functions which is exact in the short-time[8] and classical limits, and for linear operators in harmonic potentials. The method has been successfully employed in a wide range of applications.[9] Application of RPMD to the simulation of electron-transfer processes, which often exhibit significant nonadiabatic character, has also been performed employing a pseudopotential approximation in which the electron is treated as a particle, without explicitly introducing electronic states.[10] The combination of this approach with electronic structure calculations is therefore not obvious. Nonetheless, RPMD was shown to provide very good results in the normal regime of electron transfer but failed in the inverted regime.

The new method proposed here, in the following referred to as nonadiabatic RPMD, employs the mapping approach, which represents the electronic states by continuous variables.[2,11–13] The nonadiabatic RPMD trajectories are initialized from an equilibrium distribution similar to that derived by Ananth and Miller[14] and evolve according to a ring-polymer Hamiltonian obtained from the mapping approach. The mapping approach has previously been applied to simulate nonadiabatic dynamics in a variety of systems employing (quasi)classical, semiclassical, centroid molecular dynamics (CMD), and other implementations.[2,12–17] Within a (quasi)classical implementation, problems with the flow of zero-point energy between the nuclear and electronic coordinates have been identified.[2] RPMD, on the other hand, is well-known to preserve the zero-point energy correctly in nuclear modes and may go some way to solving this problem without the need to adjust the zero-point energy.[15] In contrast to the recently proposed ring-polymer surface-hopping approach,[18] the nonadiabatic RPMD method introduced here treats electronic and nuclear motion on the same dynamical footing, which has been shown to be of advantage in previous applications of the mapping approach.[2]

MAPPING REPRESENTATION

To facilitate the outline of the nonadiabatic RPMD method, we first review briefly the basic idea of the mapping approach to nonadiabatic quantum dynamics.[2,12,13] We consider a system with L electronic states and, for notational simplicity, a single vibrational mode described by the following Hamiltonian in the diabatic representation:

$$\hat{H} = \frac{\hat{p}^2}{2m} + V_0(\hat{x}) + \sum_{n,m=1}^{L} |\phi_n\rangle \, [\mathsf{V}(\hat{x})]_{nm} \, \langle\phi_m| \,, \qquad (1)$$

where x and p are the nuclear positions and momenta, m is the nuclear mass, $V_0(x)$ is a state-independent potential, and

$\mathsf{V}(x)$ is the diabatic potential matrix in the basis of electronic states $|\phi_n\rangle$.

Within the mapping approach, each of the electronic states $|\phi_n\rangle$ can be rigorously mapped[12] onto a particular set of L harmonic oscillator eigenstates $|n\rangle \equiv |0_1, \dots, 1_n, \dots, 0_L\rangle$ referred to as a singly excited oscillator (SEO) state and given in the continuous (dimensionless) position and momentum representations by

$$\langle \mathsf{X}|n\rangle = \frac{\sqrt{2}}{\pi^{L/4}}\,[\mathsf{X}]_n\,\mathrm{e}^{-\frac{1}{2}|\mathsf{X}|^2}, \quad \langle \mathsf{P}|n\rangle = \frac{-\mathrm{i}\sqrt{2}}{\pi^{L/4}}\,[\mathsf{P}]_n\,\mathrm{e}^{-\frac{1}{2}|\mathsf{P}|^2},$$

where $[\mathsf{X}]_n$ and $[\mathsf{P}]_n$ are elements of the vectors X and P.

The Hamiltonian in the mapping representation, equivalent to that of Eq. (1), is defined as[11,12]

$$\hat{\mathcal{H}} = \frac{\hat{p}^2}{2m} + \hat{\mathcal{V}}, \tag{2}$$

where

$$\hat{\mathcal{V}} = V_0(\hat{x}) + \tfrac{1}{2}\big[\hat{\mathsf{X}}^\mathsf{T}\mathsf{V}(\hat{x})\hat{\mathsf{X}} + \hat{\mathsf{P}}^\mathsf{T}\mathsf{V}(\hat{x})\hat{\mathsf{P}} - \mathrm{tr}\,\mathsf{V}(\hat{x})\big]. \tag{3}$$

The mapping provides a representation of the discrete electronic states in terms of continuous variables which is exact on the quantum-mechanical level of theory.

For later use, we note that there is a certain degree of freedom in the choice of separation into state-independent and state-dependent parts of the potential which does not affect the quantum-mechanical result or the short-time limit of the proposed method. However, for what follows, we recommend the choice be made to force the lowest eigenvalue of $\mathsf{V}(x)$ to be zero everywhere, as this greatly improves the convergence of the sampling within the nonadiabatic RPMD method.

FORMULATION OF THE NONADIABATIC RPMD METHOD

Following a similar derivation to that of standard RPMD,[8] we begin by deriving exact expressions for static quantities using a discretized path-integral approach,[7] in this case using the mapping representation of the electronic states. This is similar to the derivation followed by Ananth and Miller[14] except that we also introduce sampling over the momenta of the mapping coordinates, which is necessary to initialize the ring-polymer mapping dynamics proposed in this paper.

The partition function $Z = \mathrm{tr}[\mathrm{e}^{-\beta\hat{\mathcal{H}}}]$ at reciprocal temperature $\beta = (k_\mathrm{B}T)^{-1}$ can be formulated in the limit of an infinite number of ring-polymer beads N, such that $\beta_N = \beta/N \to 0$, by inserting identities of nuclear position states and position and momenta mapping states, ensuring the correct projection onto the finite subspace of SEOs.[14]

$$\begin{aligned} Z \simeq \mathrm{tr}\Bigg[\prod_{i=1}^{N}\sum_{k,l,m,n=1}^{L}\iiint_{-\infty}^{\infty} &|k\rangle\,\langle k|\mathsf{X}_i\rangle\,\langle \mathsf{X}_i|l\rangle\,\langle l|\,\mathrm{e}^{-\beta_N\hat{\mathcal{V}}/2} \\ &\times |x_i\rangle\,\langle x_i|\,\mathrm{e}^{-\beta_N\hat{p}^2/2m}\,|m\rangle\,\langle m|\mathsf{P}_i\rangle\,\langle \mathsf{P}_i|n\rangle\,\langle n| \\ &\times \mathrm{e}^{-\beta_N\hat{\mathcal{V}}/2}\,\mathrm{d}x_i\,\mathrm{d}\mathsf{X}_i\,\mathrm{d}\mathsf{P}_i\Bigg] \end{aligned} \tag{4a}$$

$$\begin{aligned} &= \iiint_{-\infty}^{\infty}\mathrm{e}^{-\beta_N U_N(\boldsymbol{x})}\prod_{i=1}^{N}\sqrt{\frac{m}{2\pi\beta_N\hbar^2}}\,\frac{4}{\pi^L}\,\mathrm{e}^{-|\mathsf{X}_i|^2-|\mathsf{P}_i|^2} \\ &\quad\times\big(\mathsf{P}_{i-1}^\mathsf{T}\mathsf{M}_i\mathsf{X}_i\big)\big(\mathsf{X}_i^\mathsf{T}\mathsf{M}_i\mathsf{P}_i\big)\,\mathrm{d}\boldsymbol{x}\,\mathrm{d}\boldsymbol{X}\,\mathrm{d}\boldsymbol{P}, \end{aligned} \tag{4b}$$

where $\boldsymbol{x} = \{x_1, \dots, x_N\}$, $\boldsymbol{X} = \{\mathsf{X}_1, \dots, \mathsf{X}_N\}$ and likewise for $\boldsymbol{p}$ and $\boldsymbol{P}$, and these subscripts refer to the bead index. The $L\times L$ matrices,

$$\mathsf{M}_i = \mathrm{e}^{-\beta_N\mathsf{V}(x_i)/2}, \tag{5}$$

can be computed using eigenvalue decomposition or more efficiently for the case of $L = 2$ using the analytical result. The standard ring-polymer potential is given by

$$U_N(\boldsymbol{x}) = \sum_{i=1}^{N} V_0(x_i) + \frac{m}{2\beta_N^2\hbar^2}(x_i - x_{i+1})^2. \tag{6}$$

The relative locations for the insertion of the mapping states in Eq. (4a) are arbitrary for the calculation of equilibrium averages, but the symmetric choice above can be shown to give the most accurate zero-time value of Eq. (12b) for a separable system with only one bead.

It is noted that the integrand of the partition function is not positive-definite except in the single-bead case. Nonetheless, we can define a probability distribution

$$\rho(\boldsymbol{x}, \boldsymbol{p}, \boldsymbol{X}, \boldsymbol{P}) \sim |W|\,\mathrm{e}^{-|\boldsymbol{X}|^2-|\boldsymbol{P}|^2-\beta_N[|\boldsymbol{p}|^2/2m+U_N(\boldsymbol{x})]}, \tag{7}$$

where

$$W \equiv W(\boldsymbol{x}, \boldsymbol{X}, \boldsymbol{P}) = \prod_{i=1}^{N}\big(\mathsf{P}_{i-1}^\mathsf{T}\mathsf{M}_i\mathsf{X}_i\big)\big(\mathsf{X}_i^\mathsf{T}\mathsf{M}_i\mathsf{P}_i\big), \tag{8}$$

which can be sampled using a Metropolis algorithm, and when corrected by the sign of W, gives true Boltzmann statistics. In the simulations, attempted moves were generated for the mapping coordinates of individual beads from the distribution $\mathrm{e}^{-|\mathsf{X}_i|^2-|\mathsf{P}_i|^2}$ and interspersed with standard path-integral Monte Carlo moves.[19]

Time-independent equilibrium quantities can be obtained from a derivation similar to that of Eqs. (4). For example, the population of the diabatic state $|\phi_n\rangle$ is computed using

$$\frac{1}{Z}\,\mathrm{tr}\big[\mathrm{e}^{-\beta\hat{\mathcal{H}}}\,|n\rangle\langle n|\big] = \frac{\langle \bar{A}_n(\boldsymbol{x}, \boldsymbol{X}, \boldsymbol{P})\,\mathrm{sgn}\,W\rangle_\rho}{\langle \mathrm{sgn}\,W\rangle_\rho}, \tag{9}$$

$$\bar{A}_n(\boldsymbol{x}, \boldsymbol{X}, \boldsymbol{P}) = \frac{1}{N}\sum_{i=1}^{N}\frac{[\mathsf{P}_{i-1}]_n[\mathsf{M}_i\mathsf{X}_i]_n}{\big(\mathsf{P}_{i-1}^\mathsf{T}\mathsf{M}_i\mathsf{X}_i\big)}, \tag{10}$$

where the angular brackets $\langle\dots\rangle_\rho$ denote an average over the distribution given in Eq. (7).

Such equilibrium averages are exact in the $N \to \infty$ limit and also with any value of N for electronic properties of Hamiltonians without vibronic coupling. Although sampling becomes more difficult for large N as the denominator tends to zero, we will show below that often only a small number of beads are needed, where for the $N = 4$ results, only about a quarter of the trajectories had negative weights. This sampling issue is lessened if the initial state is approximately adiabatic[20] and has no bearing on the scaling to larger systems.

Of course, these static quantities could be computed in a much simpler manner employing the original representation of the Hamiltonian with discrete electronic states.[21] However, the real-time dynamics cannot be performed in this way because, although in the adiabatic limit they tend correctly to standard RPMD, transitions would erroneously be allowed between electronic states where the electronic coupling is zero. This stems from the neglect of Rabi oscillations in such a Boltzmann-weighted mean-field approach. To describe real-time dynamics, the proposed nonadiabatic RPMD method uses equations of motion derived from the following ring-polymer mapping Hamiltonian:

$$\begin{aligned}\mathcal{H}_N(\boldsymbol{x}, \boldsymbol{p}, \boldsymbol{X}, \boldsymbol{P}) &= \frac{|\boldsymbol{p}|^2}{2m} + U_N(\boldsymbol{x}) \\ &\quad + \sum_{i=1}^{N} \tfrac{1}{2}\left[\mathsf{X}_i^{\mathsf{T}}\mathsf{V}(x_i)\mathsf{X}_i + \mathsf{P}_i^{\mathsf{T}}\mathsf{V}(x_i)\mathsf{P}_i - \mathrm{tr}\,\mathsf{V}(x_i)\right]. \quad (11)\end{aligned}$$

The equations of motion preserve the total electronic population of each bead, $\frac{1}{2}(|\mathsf{X}_i|^2 + |\mathsf{P}_i|^2 - L)$, and it is noted that the coupling between the electronic coordinates of different beads is provided only through the ring-polymer springs on the nuclei.

The proposed method provides approximations to the Kubo-transformed thermal correlation functions,

$$\tilde{C}_{AB}(t) = \frac{1}{Z\beta}\int_0^\beta \mathrm{tr}\left[\mathrm{e}^{-(\beta-\lambda)\hat{H}}\hat{A}\mathrm{e}^{-\lambda\hat{H}}\mathrm{e}^{\mathrm{i}\hat{H}t/\hbar}\hat{B}\mathrm{e}^{-\mathrm{i}\hat{H}t/\hbar}\right]\mathrm{d}\lambda.$$

In this paper, we consider specifically the two cases of the autocorrelation functions of the nuclear position, $\hat{A} = \hat{B} = \hat{x}$, and the electronic population, $\hat{A} = \hat{B} = |\phi_n\rangle\langle\phi_n|$. The appropriate ring-polymer correlation functions are

$$\tilde{C}_{xx}(t) \approx \frac{\langle \bar{x}_0\, \bar{x}_t\ \mathrm{sgn}\, W(\boldsymbol{x}_0, \boldsymbol{X}_0, \boldsymbol{P}_0)\rangle_\rho}{\langle \mathrm{sgn}\, W(\boldsymbol{x}_0, \boldsymbol{X}_0, \boldsymbol{P}_0)\rangle_\rho}, \quad (12a)$$

$$\tilde{C}_{nn}(t) \approx \frac{\langle \bar{A}_n(\boldsymbol{x}_0, \boldsymbol{X}_0, \boldsymbol{P}_0)\bar{B}_n(\boldsymbol{X}_t, \boldsymbol{P}_t)\,\mathrm{sgn}\, W(\boldsymbol{x}_0, \boldsymbol{X}_0, \boldsymbol{P}_0)\rangle_\rho}{\langle \mathrm{sgn}\, W(\boldsymbol{x}_0, \boldsymbol{X}_0, \boldsymbol{P}_0)\rangle_\rho}, \quad (12b)$$

where the subscripts give the time along the trajectories and the centroids of the variables are defined by

$$\bar{x} = \frac{1}{N}\sum_{i=1}^{N} x_i, \quad (13)$$

$$\bar{B}_n(\boldsymbol{X}, \boldsymbol{P}) = \frac{1}{N}\sum_{i=1}^{N} \tfrac{1}{2}\left([\mathsf{X}_i]_n^2 + [\mathsf{P}_i]_n^2 - 1\right), \quad (14)$$

where, in the latter, we have made use of the mapping relation $|\phi_n\rangle\langle\phi_n| \to \frac{1}{2}(\hat{\mathsf{X}}_n^2 + \hat{\mathsf{P}}_n^2 - 1)$.[22]

The correlation functions are evaluated using the same methods used in classical mechanics and standard RPMD. First, values of $\boldsymbol{x}_0$, $\boldsymbol{X}_0$, and $\boldsymbol{P}_0$ are selected from a Metropolis simulation, whereas $\boldsymbol{p}_0$ is chosen from a multidimensional normal distribution. Trajectories are then run from these initial values using a velocity Verlet scheme, taking advantage of analytical updates for both the free ring-polymer normal modes and the harmonic mapping coordinate motions.

In the separable case where V is independent of x, the electronic and nuclear degrees of freedom are independent and Eq. (12b) converges, in the large N limit, to the exact analytic quantum result. The correct Rabi frequency is recovered in both the classical (single-bead) and ring-polymer versions. However unlike the computation of population probabilities,[13] it is necessary, just as with semiclassical methods,[14] to use multiple beads in order to compute the correct amplitude of this thermal autocorrelation function of a nonlinear operator.

Due to the lowest eigenvalue of $\mathsf{V}(x)$ (the adiabatic surface) being zero, Eq. (12a) tends to standard RPMD in the adiabatic limit and thus the Born-Oppenheimer approximation is automatically recovered where valid. There are, however, cases where a different potential separation in Eq. (11) may be advantageous, such as $\mathrm{tr}\,\mathsf{V}(x) = 0$ for systems with very weak electronic coupling in the region of an avoided crossing. In fact, in this case, for a system like Eq. (15) with $\Delta = 0$, Eqs. (12) give exact results for any N. Either way, the short-time results are not affected, and in the following calculations, we will employ the former definition.

RESULTS

For illustration of the performance of the new method, we consider a system with two electronic states and a single vibrational mode, modelling, e.g., a vibrationally coupled electron-transfer process between a donor and acceptor state:

$$\hat{H} = \frac{\hat{p}^2}{2m} + \tfrac{1}{2}m\omega^2\hat{x}^2 + \begin{pmatrix}\alpha + \kappa\hat{x} & \Delta \\ \Delta & -\alpha - \kappa\hat{x}\end{pmatrix}. \quad (15)$$

Thereby, Δ is the electronic coupling, κ is the vibronic coupling, and 2α is the energy bias. Reduced units are used such that m and $\hbar$ are equal to 1, and by setting the frequency $\omega = 1$, we effectively measure energy in units of ω. To facilitate comparison with Ref. 14, where this model was considered, we chose $\kappa = 1$, $\beta = 1$, and unless stated otherwise, $\alpha = 0$. Correlation functions were computed for three nonseparable systems and compared with numerically exact quantum results from a discrete-variable representation (DVR) calculation.

For strong electronic coupling, $\Delta = 4$, the timescale of the electronic oscillations is much shorter than that of the nuclear dynamics, such that the nuclei move in a mean field of the diabatic surfaces. This is close to the adiabatic limit where the nuclear dynamics tend to standard RPMD, which is shown in Fig. 1(a), are almost exact in this case as $V_0(x)$ is approximately harmonic.[8] The proposed nonadiabatic RPMD method, converged with four beads, also provides an excellent approximation to the electronic correlation function, which only degrades slightly after a few oscillations, and is a significant improvement over the single-bead result.

With the parameters $\alpha = 2$ and $\Delta = 1$, the system enters the inverted Marcus regime. The major dynamical effects can be captured with the proposed method as shown in Fig. 1(b), where again at least four beads are needed to describe them accurately. It is seen that the equilibrium population of the

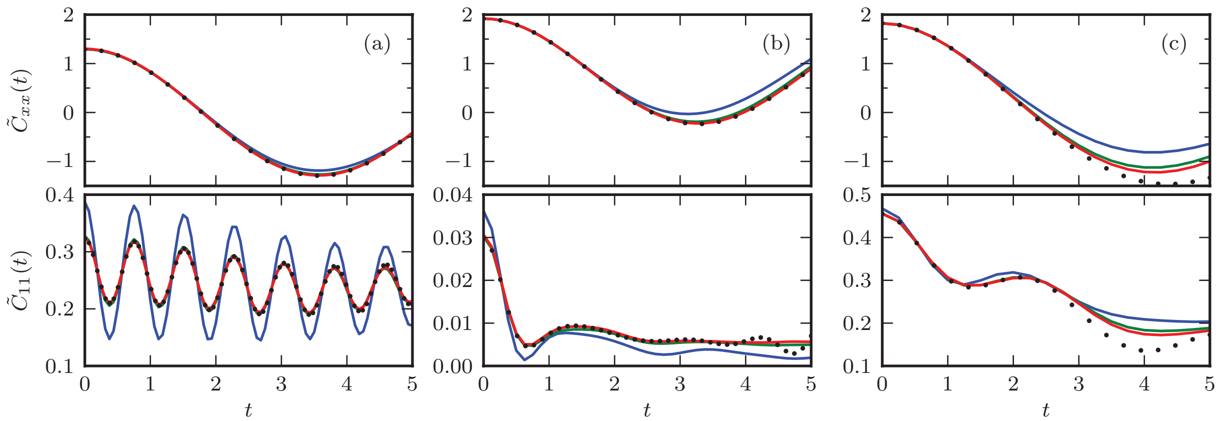

FIG. 1. Calculated correlation functions, Eqs. (12), for three systems with $\kappa = 1$ and $\beta = 1$: (a) close to the adiabatic limit with $\alpha = 0$ and $\Delta = 4$; (b) with a strong bias, $\alpha = 2$ and $\Delta = 1$; (c) in an intermediate regime with $\alpha = 0$ and $\Delta = 1$; compared with the DVR results (black dots). The blue, green, and red lines show the results of one, four, and eight bead calculations.

$|\phi_1\rangle$ state is much reduced in this case and is quickly lost to the lower-energy $|\phi_2\rangle$ state. The position autocorrelation function also shows that the system remains almost entirely on only one diabatic surface, but only with $N \geq 4$ is the method able to predict the correct amount of anharmonicity.

We finally consider a more challenging intermediate system with $\Delta = 1$ but without bias such that the timescales of the nuclear and electronic vibrations are similar. As seen in Fig. 1(c), short-time results correct to within graphical accuracy are obtained with at least four beads. The approximation does however degrade after the first electronic oscillation, although this can be improved slightly using eight beads. The comparison of the RPMD results with the (non-Kubo-transformed) semiclassical initial-value representation (SC-IVR) calculations of Ref. 14 shows that nonadiabatic RPMD is a great improvement over the linearized form (LSC-IVR) and comparable in accuracy to the Herman-Kluk IVR (for the available data). The latter approach is, however, far more computationally expensive due to phase oscillations depending on the trajectories.

CONCLUSIONS

In this paper, we have proposed a novel method that extends RPMD to the simulation of nonadiabatic dynamics by employing the mapping approach to incorporate the electronic degrees of freedom. The results show that the nonadiabatic RPMD method performs well in all regimes tested and tends to the exact or at least standard RPMD results in a number of limiting cases. It was also found to consistently improve upon the classical (single-bead) implementation of the mapping approach, presumably because of its accuracy of the short-time limit and better conservation of the SEO subspace and Boltzmann distribution.

As in the cases of the classical mapping approach, LSC-IVR or standard RPMD, the method will not provide correct long-time results in systems where nuclear quantum coherences play an important role, and we should expect it to be subject to the usual RPMD limitations such as causing spurious frequencies to appear in vibrational spectra.[9] However, the accurate treatment of electronic coherences and the short-time accuracy of the coupled dynamics should facilitate the description of rate constants[23] for nonadiabatic processes, in particular electron-transfer reactions in complex condensed-phase molecular systems, which will be the subject of future work.

ACKNOWLEDGMENTS

M.T. thanks the Chemistry Department at the University of California, Berkeley for its hospitality and a visiting Pitzer Professorship.

[1] *Conical Intersections: Electronic Structure, Dynamics and Spectroscopy*, edited by W. Domcke, D. R. Yarkony, and H. Köppel (World Scientific, Singapore, 2004).
[2] G. Stock and M. Thoss, Adv. Chem. Phys. **131**, 243 (2005).
[3] B. G. Levine and T. J. Martínez, Annu. Rev. Phys. Chem. **58**, 613 (2007).
[4] W. H. Miller, J. Phys. Chem. A **113**, 1405 (2009).
[5] J. C. Tully, J. Chem. Phys. **137**, 22A301 (2012).
[6] For an overview see the reviews 2–5 and references therein.
[7] D. Chandler and P. G. Wolynes, J. Chem. Phys. **74**, 4078 (1981).
[8] I. R. Craig and D. E. Manolopoulos, J. Chem. Phys. **121**, 3368 (2004); B. J. Braams and D. E. Manolopoulos, *ibid.* **125**, 124105 (2006).
[9] S. Habershon, D. E. Manolopoulos, T. E. Markland, and T. F. Miller III, Annu. Rev. Phys. Chem. **64**, 387 (2013).
[10] A. R. Menzeleev, N. Ananth, and T. F. Miller III, J. Chem. Phys. **135**, 074106 (2011); J. S. Kretchmer and T. F. Miller III, *ibid.* **138**, 134109 (2013).
[11] H.-D. Meyer and W. H. Miller, J. Chem. Phys. **70**, 3214 (1979).
[12] G. Stock and M. Thoss, Phys. Rev. Lett. **78**, 578 (1997).
[13] X. Sun, H. Wang, and W. H. Miller, J. Chem. Phys. **109**, 7064 (1998); H. Wang, X. Song, D. Chandler, and W. H. Miller, *ibid.* **110**, 4828 (1999).
[14] N. Ananth and T. F. Miller III, J. Chem. Phys. **133**, 234103 (2010).
[15] U. Müller and G. Stock, J. Chem. Phys. **108**, 7516 (1998); **111**, 77 (1999).
[16] J.-L. Liao and G. A. Voth, J. Phys. Chem. B **106**, 8449 (2002).
[17] S. Bonella and D. F. Coker, J. Chem. Phys. **118**, 4370 (2003); H. Kim, A. Nassimi, and R. Kapral, *ibid.* **129**, 084102 (2008); P. Huo and D. F. Coker, *ibid.* **135**, 201101 (2011).
[18] P. Shushkov, R. Li, and J. C. Tully, J. Chem. Phys. **137**, 22A549 (2012).
[19] D. M. Ceperley, Rev. Mod. Phys. **67**, 279 (1995).
[20] J. R. Schmidt and J. C. Tully, J. Chem. Phys. **127**, 094103 (2007).
[21] M. H. Alexander, Chem. Phys. Lett. **347**, 436 (2001).
[22] The CMD diabatic projection operator, $\bar{B}_n = \frac{1}{2}\left([\bar{\mathsf{X}}]_n^2 + [\bar{\mathsf{P}}]_n^2 - 1\right)$, with $\bar{\mathsf{X}}$ and $\bar{\mathsf{P}}$ defined like Eq. (13), leads to incorrect results as it is well known that nonlinear operators treated in this way give rise to higher-order Kubo transforms. See D. R. Reichman, P.-N. Roy, S. Jang, and G. A. Voth, J. Chem. Phys. **113**, 919 (2000).
[23] J. O. Richardson and S. C. Althorpe, J. Chem. Phys. **131**, 214106 (2009); T. J. H. Hele and S. C. Althorpe, *ibid.* **138**, 084108 (2013).